

# Remarks on some typical assumptions in dynamo theory<sup>1</sup>

FRIEDRICH H. BUSSE<sup>†\*</sup> and RADOSTIN D. SIMITEV<sup>‡</sup><sup>†</sup>Institute of Physics, University of Bayreuth, D-95440 Bayreuth, Germany<sup>‡</sup>School of Mathematics and Statistics, University of Glasgow, G12 8QW Glasgow, UK

(June 3, 2018)

Some concepts used in the theory of convection-driven dynamos in rotating spherical fluid shells are discussed. The analogy between imposed magnetic fields and those generated by dynamo action is evaluated and the role of the Elsasser number is considered. Eddy diffusivities are essential ingredients in numerical dynamo simulations, but their effects could be misleading. New aspects of the simultaneous existence of different dynamo states are described.

Keywords: Convection-driven dynamos; Elsasser number; Eddy diffusivities; Multiplicity of turbulent states

## 1 Introduction

Magnetohydrodynamic turbulence, i.e. hydrodynamic turbulence together with dynamo generated magnetic fields, is a particularly complex phenomenon that is still far from being fully understood. This is hardly surprising in view of the fact that the number of degrees of freedom is roughly doubled in comparison with its purely hydrodynamic version. The complexities of the details of MHD-turbulence stand in stark contrast to the observed simple structures such as planetary dipolar fields nearly aligned with the axis of rotation or the solar magnetic cycle with its surprisingly regular period of 22 years. It is thus understandable that numerous attempts have been made to find simple balances or to devise simplifying concepts in order to gain some understanding of the dynamics of MHD-turbulence.

In the following the validity of some of the assumptions that have been widely used in dynamo theory will be discussed. We shall restrict ourselves to buoyancy-driven motions which are responsible for the generation of planetary and stellar magnetic fields and even within this restricted field no completeness will be attempted.

## 2 Dynamo generated magnetic fields versus imposed fields

The simplest approach for analyzing magnetohydrodynamic phenomena is the consideration of the dynamics of an electrically conducting fluid in the presence of an imposed magnetic field  $\mathbf{B}_0$ . This approach has been used by several theoreticians and experimenters in the period from approximately 1950 to 1970 in order to understand the onset of thermal convection in the presence of a uniform imposed  $\mathbf{B}_0$ . An account of these efforts can be found in Chandrasekhar's (1961) famous treatise. In later years nonlinear aspects of the interaction between convection and the imposed magnetic field have been studied. We refer to the review of Proctor and Weiss (1982).

Of special interest is the role of magnetic fields in the case of convection in a rotating system. As described in Chandrasekhar's (1961) book the onset of convection is strongly inhibited in systems with a vertical axis

---

\*Corresponding author. Email: busse@uni-bayreuth.de

<sup>1</sup>Dedicated to Raymond Hide on the occasion of his 80th birthday.

of rotation or, in a non-rotating system, by an imposed vertical magnetic field when the fluid is electrically conducting. The critical value  $R_c$  of the Rayleigh number  $R$  for onset of convection thus increases with the 4/3-power of the Coriolis number  $\tau$  in the non-magnetic system while it increases in proportion to the Chandrasekhar number  $Q$  in a non-rotating system. But in systems with both a vertical axis of rotation and an applied vertical magnetic field the onset of convection is facilitated by the counteracting effects of the Coriolis force and Lorentz force such that  $R_c$  may increase only linearly with  $\tau$  (Eltayeb 1972). The dimensionless parameters introduced here and the ordinary and magnetic Prandtl numbers are defined by

$$R = \frac{\alpha g \Delta T d^3}{\nu \kappa}, \quad \tau = \frac{2\Omega d^2}{\nu}, \quad Q = \frac{B_0^2 d^2}{\mu \rho \lambda \nu}, \quad P = \frac{\nu}{\kappa}, \quad P_m = \frac{\nu}{\lambda}, \quad (1)$$

where  $B_0, \Omega, \mu, \nu, \kappa, \rho$  and  $\lambda$  denote the flux density of the applied magnetic field, the angular velocity of rotation, the magnetic permeability, the kinematic viscosity, the thermal diffusivity, the density and the magnetic diffusivity, respectively.  $\Delta T$  is the applied temperature difference between the boundaries and  $d$  is the distance between them;  $\alpha$  is the coefficient of thermal expansion and  $g$  is the acceleration of gravity. The inverse of  $\tau$  is also known as the Ekman number.

The optimal balance between the Coriolis force and the Lorentz force which minimizes  $R_c$  is determined by the condition that the Elsasser number  $\Lambda$  which describes the ratio between the two forces,

$$\Lambda = \frac{B_0^2}{2\Omega \mu \rho \lambda}, \quad (2)$$

assumes a value of the order unity (Chandrasekhar 1961). The counteracting effect of rotation and magnetic field also operates when both, the axis of rotation and the imposed magnetic field, are horizontal, but directed in different direction. This situation is approximately satisfied in the equatorial region of a rotating spherical fluid shell. For a zonal magnetic field the onset of convection in this case has been studied numerically by Fearn (1979). In the closely related configuration of the rotating annulus with decreasing height with distance from the axis analytical expressions for the critical Rayleigh number and the associated wavenumber can be obtained (Busse 1983). Both, the numerical and the analytical results agree quite well and exhibit a minimum critical Rayleigh number for  $\Lambda \approx 1$ .

Because of the special role played by the Elsasser number in determining the optimal conditions for the onset of convection in the parameter space spanned by the rate of rotation and the imposed magnetic flux density, it seemed obvious that the condition  $\Lambda \approx 1$  may determine the strength of the observed planetary magnetic fields. This idea was proposed by Eltayeb and Roberts (1970) and it seems to work fairly well in the cases of geomagnetism and Jovian magnetism. But the numerous numerical simulations of convection-driven dynamos in rotating spherical shells have not supported this hypothesis. First of all, the increase in the size of convection rolls that is the basic reason for the reduction of the critical Rayleigh number for  $\Lambda \approx 1$  is hardly noticeable when convection flows with a dynamo field are compared with flows at the same external conditions, but without a magnetic field. This has been observed in the work of Christensen *et al.* (1999) and is also evident from the streamlines in the equatorial plane shown for different cases in figure 1. (The distinction between MD- and FD-dynamos will be discussed in section 4.) At higher values of the Coriolis number  $\tau$  some small increase in the scale of convection may be noticed in turning from the non-magnetic to the dynamo state, but this increase could be attributed to the higher amplitude of convection which also influences its characteristic scale. All figures presented in this paper are original and have been generated from numerical results based on equations (A.1) given in the Appendix. More details on the dynamo simulations can be obtained from the papers of Simitev and Busse (2005, 2007).

Both the imposed magnetic field with  $\Lambda \approx 1$  and the magnetic field generated by dynamo action do promote convection and increase the convective heat transport. The dynamo field accomplishes this mainly by putting the brakes onto the differential rotation which, although generated by the Reynolds stresses of convection, exerts an inhibiting influence on the convection eddies through its shearing action. This nonlinear process is very different from the effect of a nearly homogeneous imposed magnetic field. While the latter enters into the linear terms of the basic equations of motion and thus reduces the Rayleigh number for onset of convection, dynamo fields have not shown such an effect. A typical impression of the

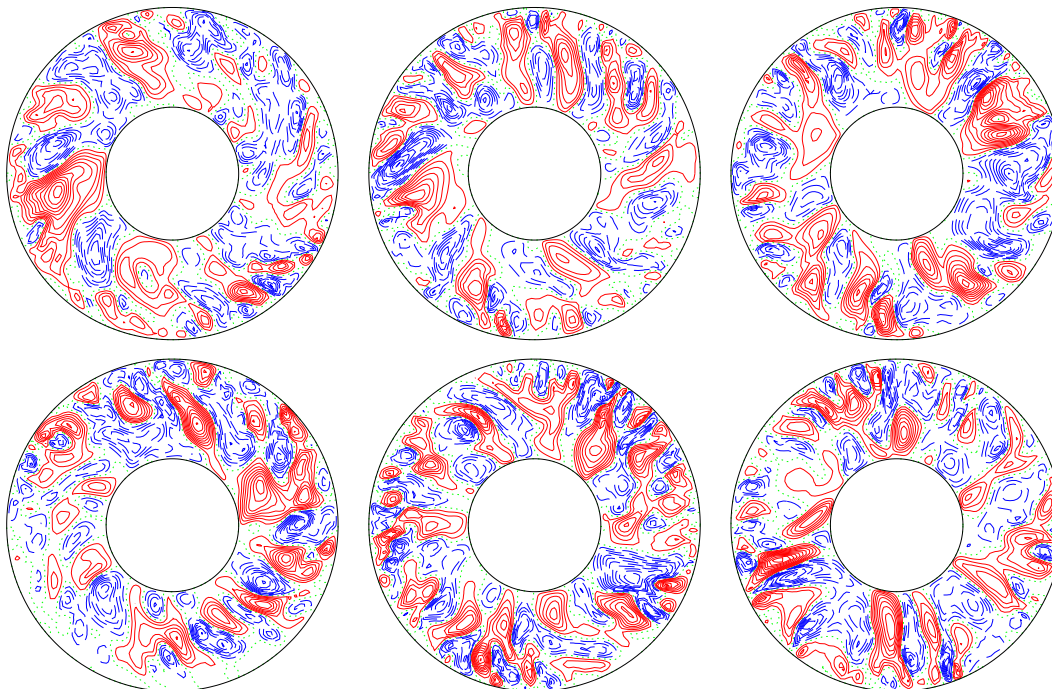


Figure 1. (Color online) Comparison of the size of convection rolls of non-magnetic convection and of self-sustained dynamo solutions. Snapshots of the equatorial streamlines  $r\partial_\varphi v = \text{const}$  at  $\tau = 3 \times 10^4$ ,  $R = 3.5 \times 10^6$  in the cases  $P = 0.5$  (first row), and  $P = 0.75$  (second row). The first plot in each row shows the non-magnetic solutions, while the second and the third plot show the FD and MD dynamo with  $P_m = 1$  (first row), and the FD and MD dynamo with  $P_m = 1.5$  (second row), respectively. (See section 4 for description of FD and MD dynamos.)

effect of the dynamo field can be gained from figure 2 where the azimuthally averaged zonal flow and the local heat transports have been plotted as a function of the colatitude  $\theta$ . These plots demonstrate that the dynamo fields affect primarily the amplitude but not the structure of convection. For the definitions of the Nusselt numbers  $Nu_i$  and  $Nu_o$  see expressions (A.7) in the Appendix.

### 3 Eddy diffusivities

Dissipation is not only an important part of all dynamical processes such as the dynamo process, but it is also an essential ingredient of most numerical schemes for the solution of nonlinear partial differential equations. Difficulties can appear when there exist large differences in the various diffusivities entering a problem. Examples are presented by the problem of high Rayleigh number convection at very low Prandtl numbers when the thermal diffusivity vastly exceeds the kinematic viscosity of the fluid or in the case of the geodynamo when it is attempted to approach the molecular values of the magnetic diffusivity and the kinematic viscosity.

For the simulation of many turbulent systems the molecular diffusivities are far too low to be used in the numerical analysis. Here the concept of eddy diffusivities enters as a convenient solution. On the one hand, it is supposed to provide a representation of the diffusive effects of small-scale turbulence that arises from those components of various fields that can not be resolved numerically. On the other hand, eddy viscosities are needed to stabilize numerical schemes. Since small scale turbulence acts in a similar fashion on many physical quantities such as momentum, magnetic flux and temperature it is usually assumed that all eddy diffusivities attain the same value and that as a consequence eddy diffusivity ratios such as the effective ordinary and magnetic Prandtl numbers can be set equal to unity.

This procedure can be misleading for several reasons. First of all, the action of turbulence on a solenoidal vector quantity tends to be different from the action on a scalar quantity. Secondly, large differences in the molecular values of diffusivities are not likely to be entirely eliminated through the effects of turbulence.

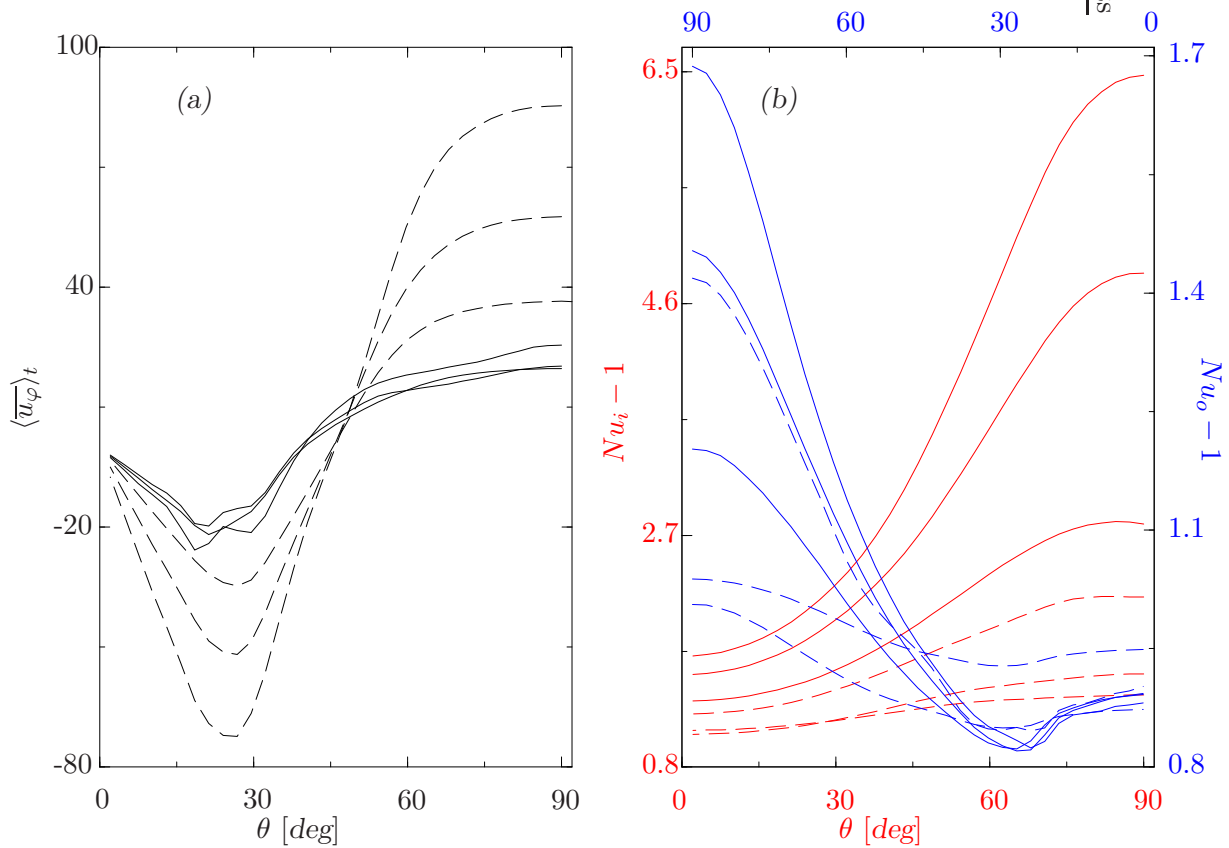


Figure 2. (Color online) Time- and azimuthally-averaged zonal flow,  $\langle \overline{u_\varphi} \rangle_t$ , at the outer spherical boundary in (a) and local  $Nu_i$  (red lines, left ordinate, lower abscissa, curves increasing to the right) and  $Nu_o$  (blue lines, right ordinate, upper abscissa, curves increasing to the left) in (b) as functions of the colatitude  $\theta$  for  $P = 1$ ,  $\tau = 10^4$ . From bottom to top at  $\theta = 90^\circ$ , the values of  $R$  are  $5 \times 10^5$ ,  $6 \times 10^5$  and  $7 \times 10^5$  for both non-magnetic convection (dashed lines) and dynamo solutions with  $P_m = 6$  (solid lines).

The Earth’s core offers an example for this problem. The molecular magnetic diffusivity is so large that its replacement by an even larger eddy diffusivity would give rise to magnetic Reynolds numbers likely to be below the critical value for dynamo action. From the property that the magnetic diffusivity by far exceeds the kinematic viscosity, it can not be concluded that the effective magnetic Prandtl number to be used in numerical simulations should be much less than unity. While usual derivations from experimental measurements (Gellert and Rüdiger 2008) and computer simulations (Yousef *et al.* 2003) yield turbulent magnetic Prandtl numbers  $P_{mt}$  in the range  $0.5 \lesssim P_{mt} \lesssim 1$ , values in excess of unity have been found (Yousef *et al.* 2003) when the molecular value of  $P_m$  was very small. In this respect the magnetic Prandtl number behaves in a similar fashion as the ordinary turbulent Prandtl number as discussed, for example, in chapter 12 of the book by Kays *et al.* (2005). In the case of liquid metals, for instance, which are characterized by a Prandtl number of the order of  $10^{-2}$ , values significantly above unity have been found for the turbulent Prandtl number  $P_t$ .

It must be kept in mind that eddy diffusivities are just crude tools for the simulation of turbulent transport processes and that a fully satisfactory determination of diffusivity ratios will never be achieved. Considerable efforts have been expended in the development of more advanced concepts of large eddy simulations (LED) in extension of methods used in non-magnetic turbulence. We refer to the work of Matsui and Buffett (2005) and of Matsushima (2005). But these efforts have been only partially successful according to the discussion by Roberts (2007). In rapidly rotating systems the use of anisotropic eddy diffusivities could lead to a more realistic description of the effects of small scale turbulence. But no systematic efforts to determine eddy diffusivity tensors have been made and in view of the doubtful concept of eddy diffusivity it is questionable whether such efforts would be worthwhile.

Finally, it should be noted that diffusivities play different roles in different situations. Turbulent Ekman layers are not well described by laminar ones with an eddy viscosity replacing the molecular value. Small

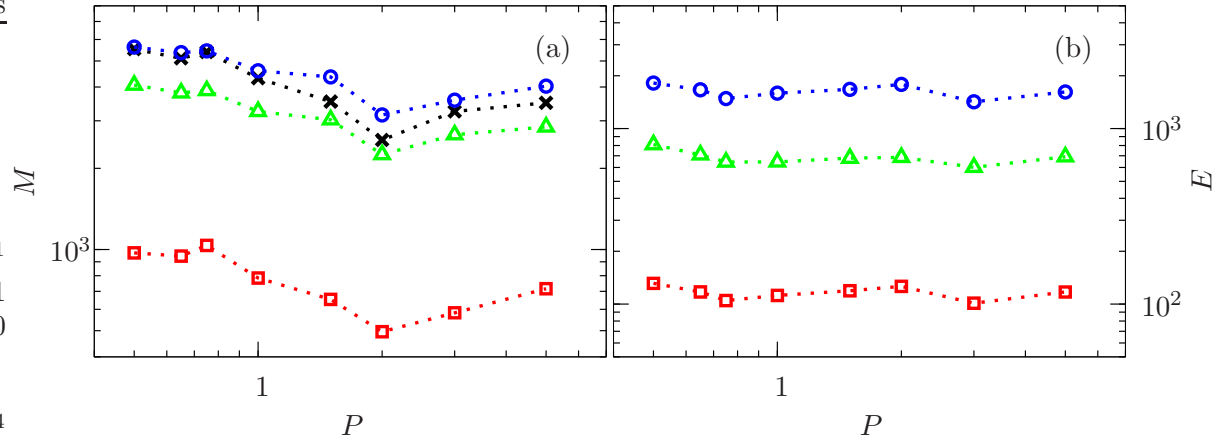


Figure 3. (Color online) Validity of the magnetostrophic approximation for MD dynamos at  $\tau = 3 \times 10^4$ ,  $R = 3.5 \times 10^6$ . Panel (a) shows the averaged magnetic energy density components multiplied by  $P$  and panel (b) shows the average kinetic energy density components multiplied by  $P^2$ , both as a function of  $P$  at fixed  $P_m/P = 2$ . In both panels, the components  $\overline{X}_p$ ,  $\overline{X}_t$ ,  $\hat{X}_p$ , and  $\hat{X}_t$  are shown by black crosses, red squares, green triangles and blue circles, respectively, where  $X = M, E$ . The energy density  $\overline{E}_p$ , has not been included in the right hand plot since it is nearly two orders of magnitude smaller than  $\overline{E}_t$ .

scale turbulence tends to cancel the effect of the Coriolis force and to modify Ekman layers into boundary layers more similar to those found in turbulent shear flows in non-rotating systems (Coleman *et al.* 1990). In a recent paper Miyagoshi *et al.* (2010) have numerically simulated convection driven dynamo in rotating spheres with a no-slip outer boundary at the very low Ekman number of  $10^{-7}$ . They have come to the conclusion that the results are more similar to those with a stress-free outer boundary than to those with a no-slip boundary together with a more commonly used Ekman number of the order  $10^{-5}$  or larger. We thus tend to conclude that the use of a stress-free boundary condition may be more realistic in simulations of the geodynamo than a no-slip boundary with a relatively thick Ekman layer attached to it.

#### 4 Parameter dependence of spherical dynamos

In spite of their shortcomings eddy diffusivities and their ratios will continue to be used in numerical dynamo simulations for the foreseeable future. We have already emphasized the importance of allowing for different values of the various eddy diffusivities. This importance is amplified by the fact that the properties of turbulent convection driven dynamos seem to vary most rapidly with  $P$  and  $P_m$  in the neighborhood where these parameters assume the value unity.

In the parameter range in which most simulations of convection driven spherical dynamos have been carried out, two basically different types of dipolar dynamos have been found. The two types can not be distinguished by their symmetry properties. Only the relative amplitudes of various components of the magnetic and the velocity fields differ greatly. One type which we shall refer to as MD-dynamo is characterized by a dominant axisymmetric dipole which in his ideal manifestation is nearly steady, but which can also oscillate in time, especially if the Rayleigh number is not very high. The other type of dynamo referred to as FD-dynamo is dominated by non-axisymmetric components of the magnetic field with their energy exceeding the energy of the axisymmetric components. Nevertheless outside the conducting spherical shell these dynamos may exhibit a nearly axisymmetric dipole which at lower Prandtl numbers may be replaced by a hemispherical or an axial quadrupolar field. For even more dominant non-axisymmetric components the outside field can sometimes be approximated by an equatorial dipole field.

In this work, the symbols MD and FD stand for “mean dipolar” and “fluctuating dipolar” as they are supposed to indicate the dominance of the mean components in the MD case while the fluctuating components predominate in the FD dynamos (Simitev and Busse 2009). The MD-dynamo is typically realized for Prandtl numbers in excess of unity (Simitev and Busse 2005). For values of  $P$  of the order

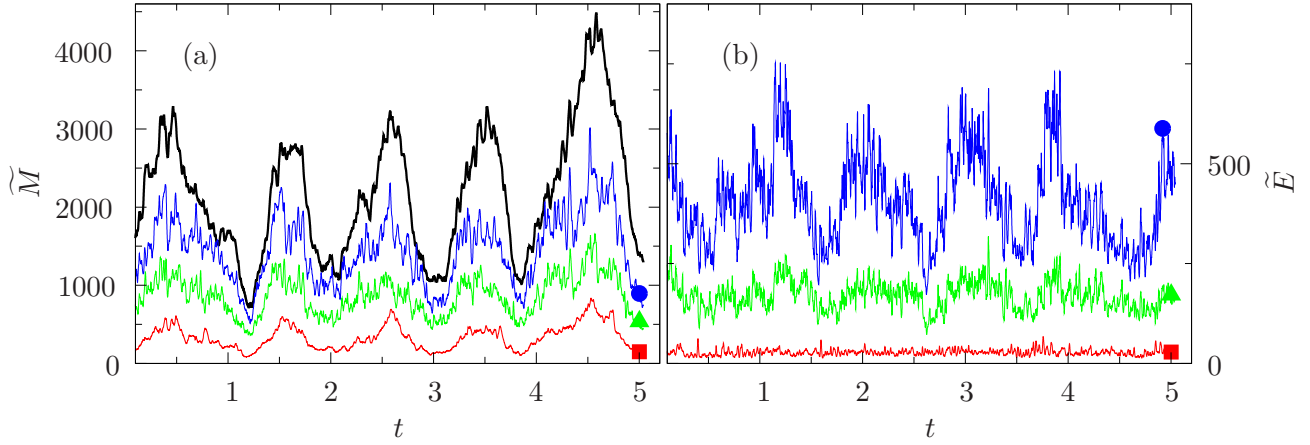


Figure 4. (Color online) MD-dynamo dipolar oscillations illustrated by the time series of the magnetic energy density components (a) and the kinetic energy density components (b) in the case  $P = 2$ ,  $\tau = 3 \times 10^4$ ,  $R = 3.5 \times 10^6$ , and  $P_m = 3$ . The component  $\overline{X}_p$  is shown by thick solid black line, while  $\overline{X}_t$ ,  $\hat{X}_p$ , and  $\hat{X}_t$  are shown by thin red, green and blue lines, respectively and they are also indicated by squares, triangles, and circles, respectively.  $X$  stands for either  $\widetilde{M}$  or  $\widetilde{E}$ .

one it can be generated if the Rayleigh number is not too high. The work of Christensen *et al.* (1999) and of Kutzner and Christensen (2002) has exhibited quite well the transition from MD-type to FD-type dynamos as a function of the Rayleigh number. As is emphasized in the latter paper, reversals of the poloidal dipolar field are only found in the narrow transition region between the two types of dynamos. This result seems to hold also for the transition region between the two types of dynamos as a function of the Prandtl number. The transition from FD- to MD-dynamos with increasing  $P$  has also been observed by Sreenivasan and Jones (2006) who assumed  $P = P_m$ . The property that both types of dynamos can exist at the same parameter values over an extended region of the parameter space has been first demonstrated by Simitev and Busse (2009).

For the MD-dynamos a description in terms of the magnetostrophic approximation can be applied since the generation of the geostrophic zonal flow by Reynolds stresses is nearly suppressed. For detailed formulations of various versions of this approximation see Simitev and Busse (2005). According to the magnetostrophic approximation the dependence of dynamos on the Prandtl number disappears. That this property is approximately satisfied for MD-dynamos is evident from figure 3, where the dependence of the components of the kinetic and magnetic energy densities are plotted as a function of the Prandtl number at fixed ratio  $P_m/P$ . The various energy density components are defined by

$$\overline{M}_p = \frac{1}{2} \langle |\nabla \times (\nabla \bar{h} \times \mathbf{r})|^2 \rangle, \quad \overline{M}_t = \frac{1}{2} \langle |\nabla \bar{g} \times \mathbf{r}|^2 \rangle, \quad (3a)$$

$$\hat{M}_p = \frac{1}{2} \langle |\nabla \times (\nabla \hat{h} \times \mathbf{r})|^2 \rangle, \quad \hat{M}_t = \frac{1}{2} \langle |\nabla \hat{g} \times \mathbf{r}|^2 \rangle, \quad (3b)$$

where the angular brackets indicate the average over the fluid shell and over time and  $\bar{h}$  refers to the azimuthally averaged component of the poloidal field  $h$ , while  $\hat{h}$  is defined by  $\hat{h} = h - \bar{h}$ . Analogous definitions apply for the kinetic energy densities as given in (A.6) with  $E$  replacing  $M$ . Non-geostrophic zonal flows of the thermal wind type are usually still present in MD-dynamos and are important for the generation of the mean toroidal field from the axial dipole field.

On the other hand, a geostrophic zonal flow plays an important role in the case of FD-dynamos and as a consequence the energies of the mean poloidal and toroidal magnetic fields are comparable although they are both small in comparison to the energies of the non-axisymmetric fields. As long as the Prandtl number is not too low and the Rayleigh number is not too high, FD-dynamos exhibit oscillations of the axisymmetric components of the field; see, for example, the paper by Busse and Simitev (2006). These oscillations assume the form of Parker's (1955) dynamo waves propagating from the equatorial plane towards higher latitudes. The oscillations manifest themselves primarily in the mean toroidal field and

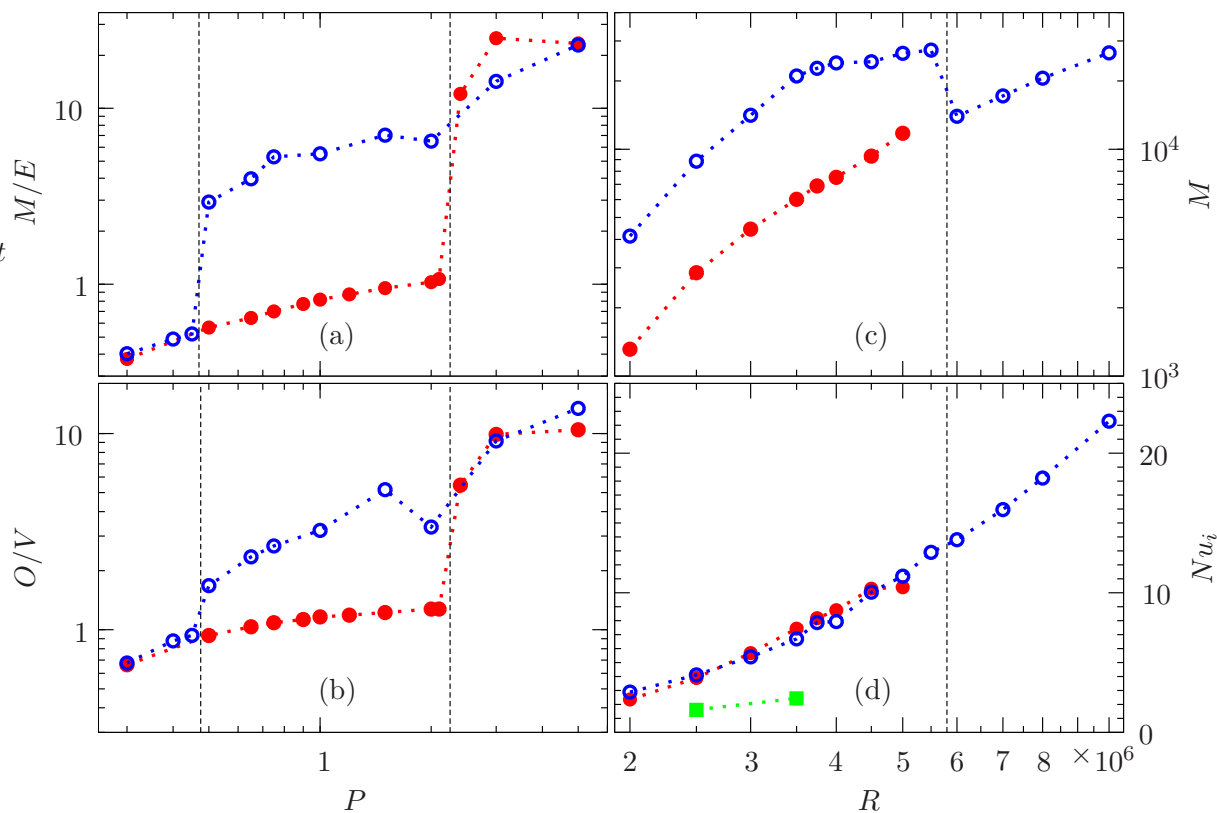


Figure 5. (Color online) Coexistence and hysteresis of MD and FD dynamos at  $\tau = 3 \times 10^4$ . Panels (a) and (b) show the ratio of the average total magnetic to the average total kinetic energy, and the ratio of the average ohmic to the average viscous dissipation, respectively, both as a function of the Prandtl number in the case of  $R = 3.5 \times 10^6$ ,  $P/P_m = 0.5$ . Panels (c) and (d) show the total magnetic energy density, and the value of the Nusselt number at  $r = r_i$ , respectively both as a function of the Rayleigh number in the case  $P = 0.75$ ,  $P_m = 1.5$ . Full red and empty blue circles indicate FD and MD dynamos, respectively. The critical value of  $R$  for the onset of thermal convection for the cases shown in (c) and (d) is  $R_c = 659145$ . Values for non-magnetic convection are indicated by green squares in (d) for comparison. Vertical dashed lines indicate the approximate transition values.

sometimes the mean poloidal field participates only in the form of variations of its amplitude without a reversal of its sign. Busse and Simatev (2008) have compared this property with the phenomenon of global excursions of the geomagnetic field which only sporadically lead to a reversal of the Earth’s dipole.

MD-dynamos can also exhibit oscillations, but these manifest themselves just in the amplitude of the various components of the velocity and the magnetic field. At relatively low Rayleigh numbers the oscillations are fairly regular with a period of the order of the viscous time scale as shown in figure 4, while at higher values of  $R$  they become more irregular.

There is, of course, no sharp boundary between the two types of dynamos and the dependence of such a not well defined boundary on the various parameters of the problem including mode of heating has not yet been investigated in detail. It appears that FD-type dynamos exist at higher values of  $P$  when the rotation rate is lowered. On the other hand, MD-dynamos tend to exist at lower Prandtl numbers when no-slip instead of stress free boundaries are used since the Ekman layer tends to damp the geostrophic zonal flow. Other types of dynamos may exist in parameter regions distinct from those that are readily accessible in present computer simulations.

## 5 Simultaneous existence of FD- and MD-dynamos

The two types of dynamos can be studied best by direct comparison in the region of the parameter space where they coexist as has been demonstrated in the paper of Simatev and Busse (2009). Here we wish to discuss further properties of the coexisting dynamos. In figure 5 the parameter range of the coexistence of FD- and MD-dynamos has been indicated in the case  $\tau = 3 \times 10^3$ . The average magnetic energy density

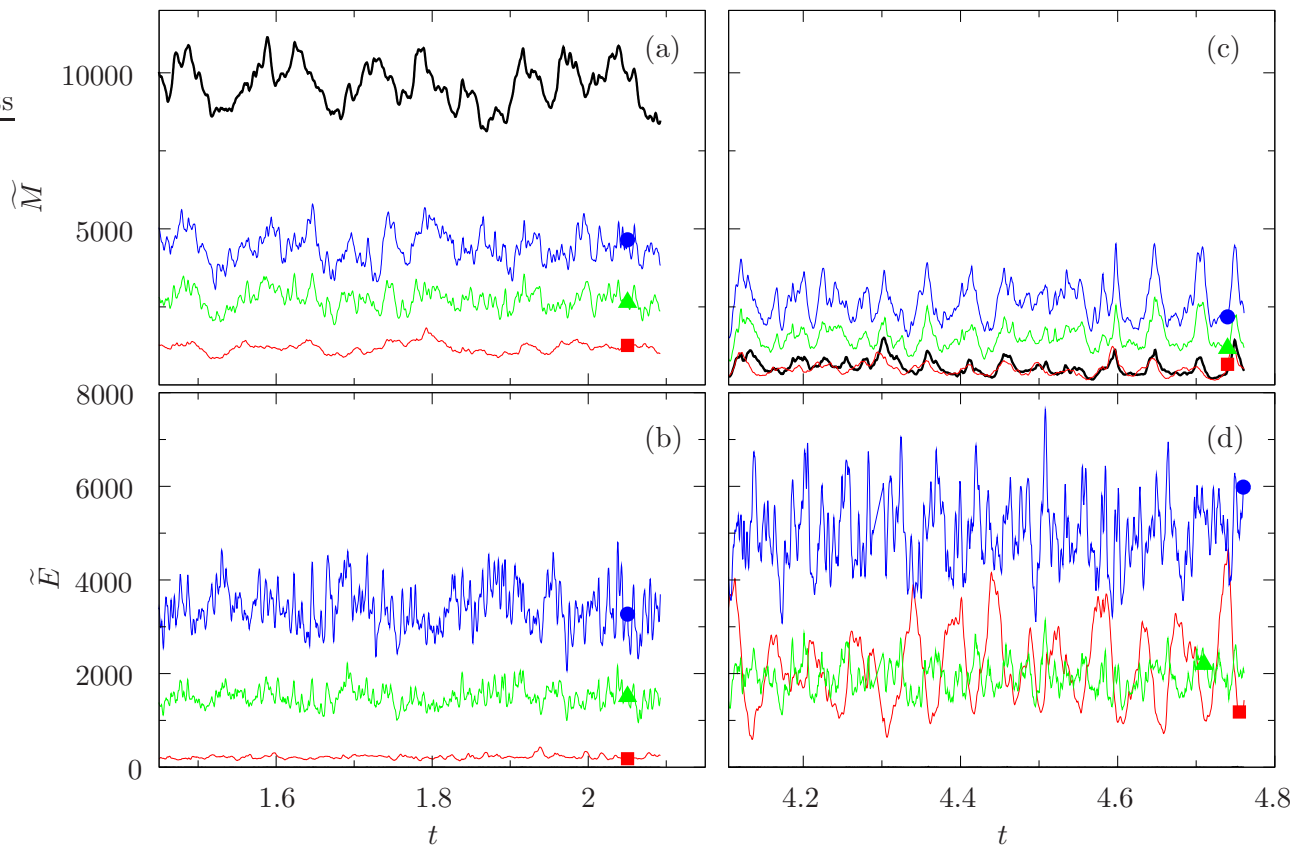


Figure 6. (Color online) Time series of two different chaotic attractors are shown – a MD (left column (a,b)) and a FD dynamo (right column (c,d)) both in the case  $R = 3.5 \times 10^6$ ,  $\tau = 3 \times 10^4$ ,  $P = 0.75$  and  $P_m = 0.75$ . The top two panels (a,c) show magnetic energy densities and the lower two panels show kinetic energy densities. The component  $\overline{X}_p$  is shown by thick solid black line, while  $\overline{X}_t$ ,  $\hat{X}_p$ , and  $\hat{X}_t$  are shown by thin red, green and blue lines, respectively, and they are also indicated by squares, triangles, and circles, respectively.  $X$  stands for either  $\tilde{M}$  or  $\tilde{E}$ .

$M$  divided by the average kinetic density  $E$  and the average ohmic dissipation divided by the average viscous dissipation,  $O/V$ , are shown as function of the Prandtl number  $P$  (for fixed  $P/P_m$  and fixed  $R$ ) on the left side of the figure. On the right side  $M$  and the Nusselt number are shown as a function of  $R$  (for fixed  $P$  and fixed  $P_m$ ). The averages are defined here as the time average of the spatial average extended over the spherical fluid shell, i.e.  $M$  is defined as the time average of  $\tilde{M} = \overline{M}_p + \hat{M}_p + \overline{M}_t + \hat{M}_t$ . The two types of dynamos differ also in characteristic ways in the energy densities of their components. These energy densities are highly chaotic as is evident from their time series shown in figure 6. Because the average energy densities in the two cases are so different, however, even large fluctuations cannot push the system from one dynamo attractor to the other.

The plot of the Nusselt number  $Nu_i$  as function of  $R$  in figure 5 demonstrates that the ability of both dynamos to attain the same maximal heat transport of convection is the basic reason for their stability. At the same time the increase of the magnetic energy density with  $R$  indicates that the available buoyancy energy rather than a constant Elsasser number determines its saturation value. This finding supports the power laws proposed by Christensen and Aubert (2006).

It is also of interest to see through which terms the various magnetic energy densities are generated. In figure 7 the various terms are shown that are obtained when the  $r$ -component of the equation of induction (A.1e) is multiplied by  $\bar{h}$  and by  $\hat{h}$  and the  $r$ -component of the curl of this equation is multiplied by  $\bar{g}$  and by  $\hat{g}$  and the results are averaged over the spherical shell. Following the procedure of Simitev and Busse (2005) we list here the most important of those terms in the sequence in which they apply in the case of

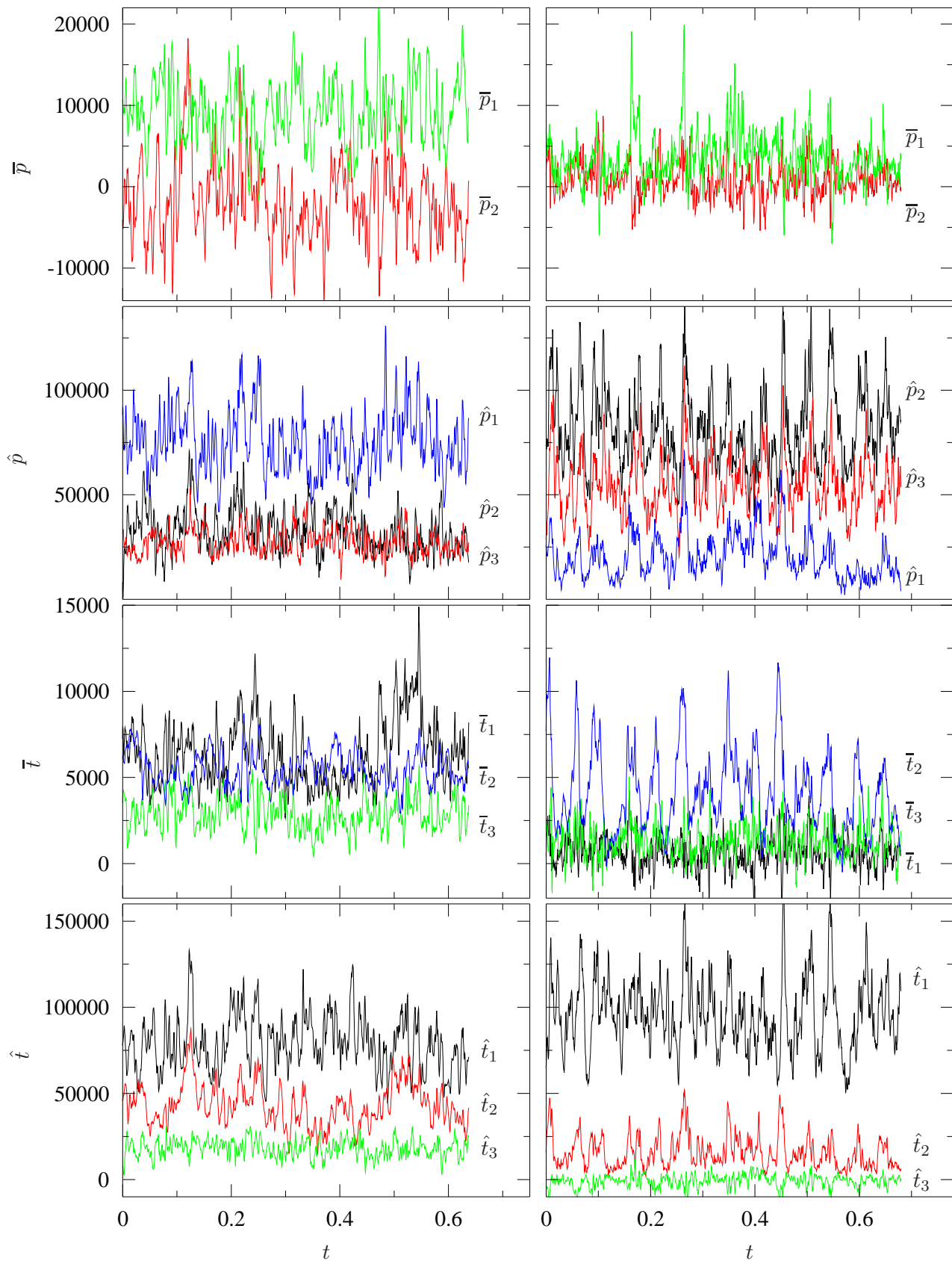


Figure 7. (Color online) Comparison of the Lorentz terms of MD (left column) and FD (right column) dynamos. Both solutions are obtained at identical parameter values  $P = 0.75$ ,  $\tau = 3 \times 10^4$ ,  $R = 3.5 \times 10^6$ , and  $P_m = 1.5$ . In the case of the FD dynamo, the mean poloidal ( $\bar{p}$ ), fluctuating poloidal ( $\hat{p}$ ) and mean toroidal terms ( $\bar{t}$ ) are multiplied by a factor of 2. The labels attached to the curves correspond to the notation introduced in formulae (4).

the MD-dynamo of figure 7,

$$\bar{p}_1 \equiv (\hat{w}\hat{h}\bar{h}), \quad \bar{p}_2 \equiv (\hat{v}\hat{g}\bar{h}), \quad (4a)$$

$$\hat{p}_1 \equiv (\hat{v}\hat{g}\hat{h}), \quad \hat{p}_2 \equiv (\hat{v}\hat{g}\hat{h}), \quad \hat{p}_3 \equiv (\hat{v}\hat{h}\hat{h}), \quad (4b)$$

$$\bar{t}_1 \equiv (\hat{v}\hat{g}\bar{g}), \quad \bar{t}_2 \equiv (\bar{w}\bar{h}\bar{g}), \quad \bar{t}_3 \equiv (\hat{w}\hat{h}\bar{g}), \quad (4c)$$

$$\hat{t}_1 \equiv (\hat{w}\hat{g}\hat{g}), \quad \hat{t}_2 \equiv (\hat{w}\hat{g}\hat{g}), \quad \hat{t}_3 \equiv (\hat{w}\bar{h}\hat{g}), \quad (4d)$$

where the first two letters inside the brackets indicate which of the interactions between velocity and magnetic field components on the right hand sides of the induction equations counteract the ohmic dissipation of the magnetic field component indicated by the last letter inside the brackets. An alternative interpretation of the averages (4) is that they represent the work done by the Lorentz forces on the components of the velocity field described by  $\bar{v}$ ,  $\hat{v}$ ,  $\bar{w}$  and  $\hat{w}$ .

In comparing the MD-results with the FD-results it is obvious that axisymmetric MD-components require higher contributions than the corresponding FD-components as can be seen from the first and third row of figure 7. (Note that FD-results of the first through third row have been multiplied by the factor two.) The FD components have smaller amplitudes and thus suffer less from ohmic dissipation. On the other hand, the non-axisymmetric toroidal field is especially strong and thus require higher (negative) work done by the Lorentz force to balance its ohmic losses. Of particular interest are the cases where the order of the amplitude of contributions given by

$$\hat{p}_2 \equiv (\hat{v}\hat{g}\hat{h}), \quad \hat{p}_3 \equiv (\hat{v}\hat{h}\hat{h}), \quad \hat{p}_1 \equiv (\hat{v}\bar{g}\hat{h}), \quad (5a)$$

$$\bar{t}_2 \equiv (\hat{w}\hat{h}\bar{g}), \quad \bar{t}_3 \equiv (\hat{v}\hat{g}\bar{g}), \quad \bar{t}_1 \equiv (\bar{w}\bar{h}\bar{g}). \quad (5b)$$

for the FD-dynamos in the case of the second and third row of figure 7 differs from the order in the case of MD-dynamos. The axisymmetric components hardly participate in the generation of the non-axisymmetric components of the FD-dynamo. On the other hand the mean toroidal field of the MD-dynamo is mainly amplified by the differential rotation stretching the mean poloidal field as suggested by the  $\alpha\omega$ -dynamo mechanism. The latter property contrasts with the results of Olson *et al.* (1999) who find little evidence for an  $\omega$ -effect. This difference can be explained by the damping of the mean zonal flow by the Ekman layer at the solid outer boundary which is absent in the case of the stress-free boundary condition (A.4) used in the present paper.

## 6 Concluding remarks

In this paper we have considered a few assumptions of dynamo theory which are often taken for granted, but which should be questioned. The difference between the effects of an imposed magnetic field and one that is generated by dynamo action is beginning to be appreciated and an Elsasser number of the order unity is no longer generally accepted for the determination of the magnetic energy equilibrium. The concept of eddy diffusivities or of similar methods for representing the effect of unresolved scales of turbulence will be needed for the foreseeable future. But the ratios of eddy diffusivities should not always be set equal to unity. Variations of these ratios can have a significant influence on convection driven dynamos and may lead to new insights in the interpretation of observed properties of planetary dynamos. Finally the common assumption of unique turbulent attractors should be abandoned and the multiplicity of turbulent states in nonlinear magnetohydrodynamics with its huge number of degrees of freedom should be appreciated. In contrast to some other cases of bistability such as the one observed in the VKS-experiment (Berhanu *et al.* 2009) the states MD and FD do not differ in their symmetry properties.

## Appendix A. Mathematical formulation of the dynamo problem

Here a brief outline of the mathematical formulation is given which is employed for the simulations of convection driven dynamos referred to in this paper. It is assumed that a static state exists with the temperature distribution  $T_S = T_0 - \beta d^2 r^2 / 2$  where  $d$  is the thickness of the spherical shell,  $rd$  is the length of the position vector with respect to the center of the sphere and the gravity field is given by  $\mathbf{g} = -d\gamma\mathbf{r}$ . In addition to the length  $d$ , the time  $d^2/\nu$ , the temperature  $\nu^2/\gamma\alpha d^4$  and the magnetic flux density  $\nu(\mu_0\varrho)^{1/2}/d$  are used as scales for the dimensionless description of the problem where  $\nu$  denotes the kinematic viscosity of the fluid,  $\kappa$  its thermal diffusivity,  $\varrho$  its density and  $\mu_0$  is its magnetic permeability. The equations of motion for the velocity vector  $\mathbf{u}$ , the heat equation for the deviation  $\Theta$  from the static temperature distribution, and the equation of induction for the magnetic flux density  $\mathbf{B}$  are thus given by

$$\partial_t \mathbf{u} + \mathbf{u} \cdot \nabla \mathbf{u} + \tau \mathbf{k} \times \mathbf{u} = -\nabla \pi + \Theta \mathbf{r} + \nabla^2 \mathbf{u} + \mathbf{B} \cdot \nabla \mathbf{B}, \quad (\text{A.1a})$$

$$\nabla \cdot \mathbf{u} = 0, \quad (\text{A.1b})$$

$$P(\partial_t \Theta + \mathbf{u} \cdot \nabla \Theta) = R \mathbf{r} \cdot \mathbf{u} + \nabla^2 \Theta, \quad (\text{A.1c})$$

$$\nabla \cdot \mathbf{B} = 0, \quad (\text{A.1d})$$

$$\nabla^2 \mathbf{B} = P_m(\partial_t \mathbf{B} + \mathbf{u} \cdot \nabla \mathbf{B} - \mathbf{B} \cdot \nabla \mathbf{u}), \quad (\text{A.1e})$$

where  $\partial_t$  denotes the partial derivative with respect to time  $t$  and where all terms in the equation of motion that can be written as gradients have been combined into  $\nabla \pi$ . The Boussinesq approximation has been assumed in that the density  $\varrho$  is regarded as constant except in the gravity term where its temperature dependence given by  $\alpha \equiv -(d\varrho/dT)/\varrho = \text{const}$  is taken into account. The dimensionless parameters obey the definitions (1) except for the Rayleigh number  $R$  which in the present spherical case is defined by

$$R = \frac{\alpha \gamma \beta d^6}{\nu \kappa}. \quad (\text{A.2})$$

Because the velocity field  $\mathbf{u}$  as well as the magnetic flux density  $\mathbf{B}$  are solenoidal vector fields, the general representation in terms of poloidal and toroidal components can be employed,

$$\mathbf{u} = \nabla \times (\nabla v \times \mathbf{r}) + \nabla w \times \mathbf{r}, \quad (\text{A.3a})$$

$$\mathbf{B} = \nabla \times (\nabla h \times \mathbf{r}) + \nabla g \times \mathbf{r}. \quad (\text{A.3b})$$

Stress-free boundaries with fixed temperatures are used,

$$v = \partial_{rr}^2 v = \partial_r(w/r) = \Theta = 0 \quad \text{at } r = r_i \equiv 2/3, \quad \text{and at } r = r_o \equiv 5/3, \quad (\text{A.4})$$

where the radius ratio is fixed at the value  $r_i/r_o = 0.4$ . For the magnetic field electrically insulating boundaries are assumed such that the poloidal function  $h$  must be matched to the function  $h^{(e)}$  which describes the potential fields outside the fluid shell

$$g = h - h^{(e)} = \partial_r(h - h^{(e)}) = 0 \quad \text{at } r = r_i \text{ and } r = r_o. \quad (\text{A.5})$$

The energy densities are defined by

$$\overline{E}_p = \frac{1}{2} \langle |\nabla \times (\nabla \bar{v} \times \mathbf{r})|^2 \rangle, \quad \overline{E}_t = \frac{1}{2} \langle |\nabla \bar{w} \times \mathbf{r}|^2 \rangle, \quad (\text{A.6a})$$

$$\hat{E}_p = \frac{1}{2} \langle |\nabla \times (\nabla \hat{v} \times \mathbf{r})|^2 \rangle, \quad \hat{E}_t = \frac{1}{2} \langle |\nabla \hat{w} \times \mathbf{r}|^2 \rangle, \quad (\text{A.6b})$$

where the angular brackets indicate the average over the fluid shell and  $\bar{v}$  refers to the azimuthally averaged component of  $v$ , while  $\hat{v}$  is defined by  $\hat{v} = v - \bar{v}$ . The Nusselt numbers at the inner and outer spherical boundaries  $Nu_i$  and  $Nu_o$  are defined by

$$Nu_i = 1 - \frac{P}{r_i R} \left. \frac{d\bar{\Theta}}{dr} \right|_{r=r_i}, \quad Nu_o = 1 - \frac{P}{r_o R} \left. \frac{d\bar{\Theta}}{dr} \right|_{r=r_o}, \quad (\text{A.7})$$

where the double bar indicates the average over the spherical surface. (The factor  $1/R$  has accidentally been dropped in previous papers of the authors.) The ratio of external heating to internal heating is given by

$$\frac{r_i^3 Nu_i}{r_o^3 Nu_o - r_i^3 Nu_i}. \quad (\text{A.8})$$

## REFERENCES

- Berhanu, M., Gallet, B., Monchaux, R., *et al.*, Bistability between a stationary and an oscillatory dynamo in a turbulent flow of liquid sodium. *J. Fluid Mech.* 2009, **641**, 217–226.
- Busse, F.H., Recent developments in the dynamo theory of planetary magnetism. *Ann. Rev. Earth Planet. Sci.* 1983, **11**, 241–268.
- Busse, F.H., and Simitev, R., Parameter dependences of convection-driven dynamos in rotating spherical fluid shells. *Geophys. Astrophys. Fluid Dyn.* 2006, **100**, 341–361.
- Busse, F.H., and Simitev, R., Toroidal flux oscillations as possible cause of geomagnetic excursions and reversals. *Phys. Earth Planet. Int.* 2008, **168**, 237–243.
- Chandrasekhar, S., *Hydrodynamic and Hydromagnetic Stability* 1961 (Oxford, Clarendon Press).
- Christensen, U.R., and Aubert, J., Scaling laws for dynamos in rotating spherical shells. *Geophys. J. Int.* 2006, **166**, 97–114.
- Christensen, U.R., Olson, P., and Glatzmaier, G.A., Numerical Modeling of the Geodynamo: A Systematic Parameter Study. *Geophys. J. Int.* 1999, **138**, 393–409.
- Coleman, G.N., Ferziger, J., and Spalart, P.R., A numerical study of the turbulent Ekman layer. *J. Fluid Mech.* 1990, **213**, 313–348.
- Eltayeb, I.A., Hydromagnetic convection in a rapidly rotating fluid layer. *Proc. R. Soc. Lond. A.* 1972, **326**, 229–254.
- Eltayeb, I.A., and Roberts, P.H., On the hydromagnetics of rotating fluids. *Astrophys. J.* 1970, **162**, 699–701.
- Fearn, D.R., Thermal and magnetic instabilities in a rapidly rotating fluid sphere. *Geophys. Astrophys. Fluid Dyn.* 1979, **14**, 103–126.
- Gellert, M., and Rüdiger, G., Eddy diffusivity from hydromagnetic Taylor-Couette flow experiments. *Phys. Rev. E* 2009, **80**, 046314.
- Kays, W., Crawford, M., and Weigand, B., *Convective Heat and Mass Transfer* 2005 (McGraw-Hill, 4th edn).
- Kutzner, C., and Christensen, U.R., From stable dipolar towards reversing numerical dynamos. *Phys. Earth Planet. Inter.* 2002, **131**, 29–45.
- Matsui, H. and Buffett, B., Sub-grid scale model for convection-driven dynamos in a rotating plane layer. *Phys. Earth Planet. Inter.* 2005, **153**, 108–123.
- Matsushima, M., A scale-similarity model for the subgrid-scale flux with application to MHD turbulence in the Earth's core. *Phys. Earth Planet. Inter.* 2005, **153**, 74–82.
- Miyagoshi, T., Kageyama, A., and Sato, T., Zonal flow formation in the Earth's core. *Nature* 2010, **463**, 793–796.
- Olson, P., Christensen, U., and Glatzmaier, G.A. Numerical modeling of the geodynamo: Mechanisms of field generation and equilibration. *J. Geophys. Res.* 1999, **104**, 10383–10404.

- Parker, E. N., Hydromagnetic dynamo models. *Astrophys. J.* 1955, **121**, 293–314.
- Proctor, M.R.E., and Weiss, N.O., Magnetoconvection. *Rep. Prog. Phys.* 1982, **45**, 1317–1379.
- Roberts, P.H., Sections 4.6 through 4.10 in *Mathematical Aspects of Natural Dynamos*, edited by E. Dormy and A. M. Soward 2007 (CRC Press, Taylor and Francis Group).
- Simitev, R. and Busse, F.H., Prandtl-number dependence of convection-driven dynamos in rotating spherical fluid shells. *J. Fluid Mech.* 2005, **532**, 365–388.
- Simitev, R. and Busse, F.H., Bistability and hysteresis of dipolar dynamos generated by turbulent convection in rotating spherical shells. *Europhysics Lett.* 2009, **85**, 19001.
- Sreenivasan, B. and Jones, C.A., The role of inertia in the evolution of spherical dynamos. *Geophys. J. Int.* 2006, **164**, 467–476.
- Yousef, T.A., Brandenburg, A., and Rüdiger, G., Turbulent magnetic Prandtl number and magnetic diffusivity quenching from simulations. *Astron. Astrophys.* 2003, **411**, 321–327.